

# HyperGALE: ASD Classification via Hypergraph Gated Attention with Learnable HyperEdges

Mehul Arora, Chirag S. Jain, Lalith Bharadwaj Baru, Kamalaker Dadi, Bapi Raju S

Brain Cognition Computation Lab

IIT Hyderabad, India

mehul.arora, chirag.jain@research.iit.ac.in

**Abstract**—Autism Spectrum Disorder (ASD) is a neurodevelopmental condition characterized by varied social cognitive challenges and repetitive behavioral patterns. Identifying reliable brain imaging-based biomarkers for ASD has been a persistent challenge due to the spectrum’s diverse symptomatology. Existing baselines in the field have made significant strides in this direction, yet there remains room for improvement in both performance and interpretability. We propose *HyperGALE*, which builds upon the hypergraph by incorporating learned hyperedges and gated attention mechanisms. This approach has led to substantial improvements in the model’s ability to interpret complex brain graph data, offering deeper insights into ASD biomarker characterization. Evaluated on the extensive ABIDE II dataset, *HyperGALE* not only improves interpretability but also demonstrates statistically significant enhancements in key performance metrics compared to both previous baselines and the foundational hypergraph model. The advancement *HyperGALE* brings to ASD research highlights the potential of sophisticated graph-based techniques in neurodevelopmental studies. The source code and implementation instructions are available at [Github](#).

**Index Terms**—ASD Classification, Hypergraphs, Graph Neural Networks, ABIDE II.

## I. INTRODUCTION

Autism Spectrum Disorder (ASD) is a complex neurodevelopmental condition characterized by challenges in social cognition and repetitive behaviors. Affecting a significant portion of the population, with a prevalence of approximately 1 in 36 children [1], ASD’s diagnosis is complicated by its heterogeneous nature and the limitations of existing diagnostic criteria. Emerging research suggests that the atypical behaviors observed in ASD may be linked to distinct patterns in functional connectivity (FC) within the brain [2] [3].

Functional connectivity represents dynamic interactions and synchronizations between various brain regions. These interactions form intricate networks that are foundational for cognitive processes and behaviors, exemplified by networks such as the Default Mode Network (DMN) and Dorsal Attention Network (DAN) [4]. The importance of these networks in ASD is increasingly recognized in contemporary research [5], underscoring the need for analytical models capable of discerning complex FC patterns associated with ASD.

Several models have been applied to understand ASD, ranging from traditional methods like SVM and Random Forest [6] to neural networks, CNNs and Transformers [7]–[11]. Graph-based methods have also been explored, retaining

complex brain information for ASD classification. However, these methods often overlook higher-order relationships in the brain’s network, focusing on dyadic interactions. This limitation is significant in the context of ASD, where the implicated brain regions can be highly variable and diverse [12].

Addressing the intricate challenges in ASD diagnosis, our research introduces *HyperGALE*, at the confluence of computational neuroscience and graph theory. Unlike traditional graph-based methods that primarily focus on pairwise interactions, *HyperGALE* utilizes hypergraph convolutions. This approach allows the model to capture high-order relationships within the brain’s network, crucial for understanding the complex and heterogeneous nature of ASD. Coupled with gated attention, *HyperGALE* not only discerns intricate patterns in functional connectivity but also provides a complex understanding of brain region interactions associated with ASD. Our key contributions are as follows:

- 1) We developed *HyperGALE*, a novel ASD classification approach utilizing modified hypergraph convolution and gated attention to identify critical brain regions implicated in ASD. Additionally, we re-implemented and compared several holistic baseline models on the ABIDE-II dataset. These comparisons are based on accuracy, AUC, sensitivity, and specificity, highlighting *HyperGALE*’s superior performance.
- 2) Our investigation into the model’s hyperparameters, such as the number of Regions of Interest (ROIs) in hyperedges and the hypergraph layer count, provided insights into their impact on *HyperGALE*’s performance. We also assessed the robustness of all models, including *HyperGALE*, through multiple runs with different initializations and dataset distributions, noting *HyperGALE*’s consistently low standard deviation in outcomes. The model’s generalization capabilities were further evidenced by employing a leave-one-site-out strategy.
- 3) The advancements in *HyperGALE* go beyond performance metrics, offering interpretative insights into ASD’s qualitative aspects through learnt hyperedges and gated attention. This bridges the gap between computational analysis and neuroscience, providing a deeper understanding of neurodevelopmental disorders such as ASD.

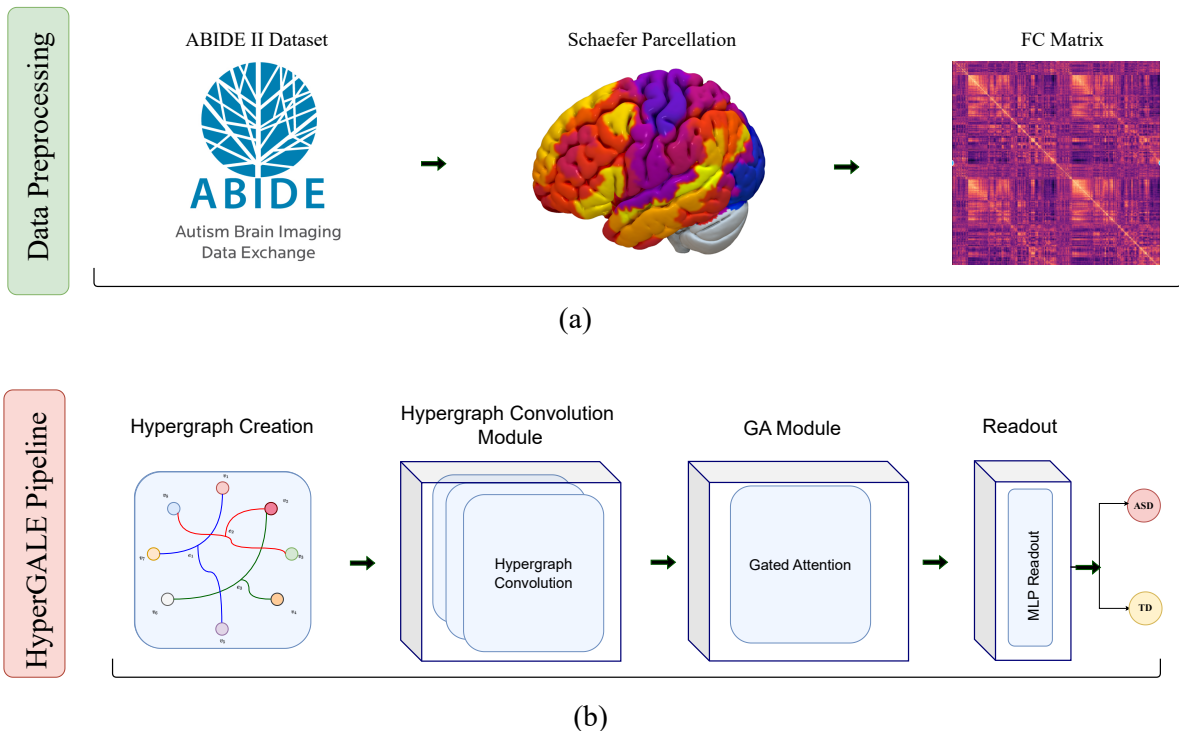


Figure 1. **ASD Processing Pipeline and the Proposed HyperGale Architecture.** (a) fMRI data is preprocessed with Schaefer’s parcellation and later converted into a functional connectivity (FC) matrix. (b) The FC matrix is then converted into a hypergraph with learnable hyperedge weights. Subsequently, the hypergraph features are sent to a series of hypergraph convolution layers and gated attention is applied in order to capture the importance of relevant information. Finally, the information extracted after attention layers is aggregated using the readout function. Finally, from these lower dimensional features of readout, a sigmoid activation leads to binary classification of ASD vs Typically Developing (TD).

## II. RELATED WORKS

In this section, we begin by briefly reviewing traditional machine-learning, deep-learning architectures that do not incorporate graph structures. We then transition to discussing the evolution and significance of graph-based and hypergraph-based methods in the context of ASD classification.

### A. Overview of Non-Graph Methods

Traditional machine learning methods, such as Support Vector Machines (SVM), Random Forests, and Gradient Boosting Classifiers (GBC) [6], have been applied to ASD classification. These methods, however, often face challenges in handling the high variance inherent in ASD data, attributed to site-specific variations and the heterogeneous nature of the disorder.

In the realm of deep learning, architectures like CNNs and Transformers have shown promise. Eslami *et al.* [8] implemented an autoencoder with data augmentation, while Kawahara *et al.* [9] utilized a CNN, treating the adjacency matrix as an image rather than exploiting its inherent graph structure. Kan *et al.* [11] innovatively employed a transformer-based approach for node embeddings with self-supervised clustering for readout.

### B. Graph-based Methods

A myriad of graph-based models was proposed on top of the standard GNNs [13], [14], [15]. For example, Cao *et al.*

[16] constructed a deep ASD diagnostic framework based on 16-layer GCN with ResNet units and DropEdge strategy to avoid certain problems such as vanishing gradient, and over-smoothing. Kazi *et al.* [17] proposes ‘inception modules’ which are capable of capturing intra- and inter-graph structural heterogeneity during convolutions. Yao *et al.* [18] introduce a multi-scale triplet graph convolutional network that employs multi-scale templates and a triplet GCN (TGCN) model to learn multi-scale graph representations of brain FC. A recent significant study by Chen *et al.* [7] put forth a competitive model that used both the resting state fMRI (brain function) and T1 weighted MRI (brain structure) to generate separate node and edge embeddings using a Transformer block.

Since the FC matrix is symmetric, traditional models tend to use the upper/lower triangular matrix features of FC, thereby lacking message passing. Therefore, these methods struggle to aggregate local and global information, resulting in poor performance. The CNNs benefit from translational equivariance and the Transformer’s key feature is the self-attention mechanism. Although, these methods have good properties, due to a lack of message passing they fail to capture aggregated neighbourhood information. Graph-based approaches on FC matrices are applied to understand interactions among regions of interest, but current methods can not take advantage of higher-order proximity information due to reliance on static dyadic edges. To address these limitations

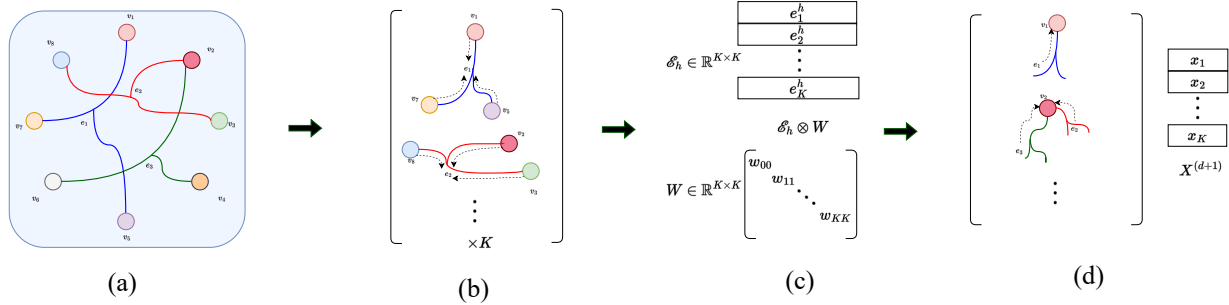


Figure 2. **Modified hypergraph convolution proposed in HyperGALE pipeline.** Starting with ROI features derived from the fully connected matrix, these initial inputs undergo node-to-hyperedge propagation to form hyperedge features (step (b)). These features are scaled using learned weights, as in step (c), the activation happens in different hyperedges with different values. Finally, the scaled hyperedge features are propagated to new node features (step (d)).

and accommodate the heterogeneity in individuals with ASD, exploring hypergraph models is considered to be a promising step.

### C. Hypergraph-based Methods

Recent ASD classification studies have explored hypergraph frameworks, such as Hypergraph U-Net [19] and multi-view HGNN [20], utilizing limited multi-modal data. Frameworks like those of Shao *et al.* [21] for Alzheimer’s classification incorporate feature selection and group-sparsity regularization in their hypergraph approach. Similarly, Liu *et al.* [22] use a view-aligned regularizer for multimodal coherence in hypergraph creation. Another notable work, [23], employs dynamic hypergraph neural networks, utilizing KNN and KMeans for iterative hypergraph generation in ASD classification.

Different from these methods, *HyperGALE* utilizes the brain’s inherent hypergraph structure with a specialized hypergraph convolution technique and learnable hyperedges. This approach enhances the interpretation of complex brain networks for more effective ASD classification.

## III. METHODOLOGY

In this section, we initially discuss each component of our method step-by-step and eventually detail the entire pipeline.

### A. Dataset and Preprocessing

To systematically benchmark various graph learning techniques for fMRI-based disease classification, we used large-scale openly-accessible fMRI dataset from ABIDE-II consortium<sup>1</sup>. This work included 812 subjects, out of which ASD: 384 and TD: 428, respectively, accumulated across 16 sites as shown on the left of Figure 4. The resting-state fMRI dataset was pre-processed using the default processing pipeline considering global signal regression and bandpass filtering implemented with C-PAC pipeline [24].

Briefly, the pre-processing pipeline included: removing the skull regions and segmentation of each anatomical image into three tissues, followed by normalization to the MNI152 template using Advanced Normalization Tools (ANTs) [25]. fMRI pre-processing included slice timing correction, motion

correction, global mean intensity normalization as well as nuisance signal regression. In nuisance signal regression, the number of parameters used were 24 parameters for head motion, CompCor [26] with five principal components signals from Cerebrospinal fluid and white matter, linear and quadratic trends for low-frequency drifts. fMRI images were then co-registered with subject-specific corresponding anatomical images and finally normalized to the MNI152 space using ANTs.

After pre-processing, timeseries signals were extracted for each node where each node belongs to 7 networks 400 parcellations from Schaefer atlas [27]. On each node time series, functional connectivity estimation using the Ledoit-Wolf regularized shrinkage estimator [28] and full correlation was implemented with Nilearn package [29].

### B. Hypergraph Modeling

As introduced earlier, we construct a graph based on the FC correlation matrix. Also, the fundamental notations and the formulations are adopted from Feng *et al.* [30]. **Basic Notations:** Suppose  $\mathcal{G} = (\mathcal{V}, \mathcal{E})$  be our graph with  $\mathcal{V}$  as vertices and  $\mathcal{E}$  edges respectively. Where,  $\mathcal{V} \in \{v_1, v_2, \dots, v_N\}$  and  $\mathcal{E} \subseteq \mathcal{V} \times \mathcal{V}$ . The Adjacency matrix  $\mathbb{A} \in \mathbb{R}^{N \times N}$  informs us of the pairwise interactions between each and every node.

Similarly, to construct a hypergraph  $\mathcal{G}_{hyper} = (\mathcal{V}, \mathcal{E}_h)$  with  $N$  nodes and  $K$  hyperedges. Similar to the adjacency matrix in the graph, in hypergraph we have *Incidence matrix*  $\mathcal{H} \in \mathbb{R}^{N \times K}$ . Here, the hyperedges  $e_j \in \mathcal{E}_h$  ( $j = 1, 2, \dots, K$ ) are dumped in a diagonal weight matrix  $W \in \mathbb{R}^{K \times K}$ . The entries in the aforementioned incidence matrix can be represented as

$$\mathcal{H}_{ij} = \begin{cases} 1 & \text{if } v_i \in e_j \\ 0 & \text{Else.} \end{cases}$$

The vertex degree and the hyperedge degree of the hypergraph are defined as  $\mathcal{D}_{ii} = \sum_{j=1}^K W_{jj} \mathcal{H}_{ij}$  and  $\mathcal{B}_{jj} = \sum_{i=1}^N \mathcal{H}_{ij}$  respectively.

**Hypergraph Convolutions:** Now, the incidence matrix  $\mathcal{H}$  is passed to a successive series of convolution layers. In order for the convolution operation to proceed the propagation is done among the shared hyperedges and higher confidence is assigned to the larger weights. Based on the hypergraph

<sup>1</sup>[http://fcon\\_1000.projects.nitrc.org/indi/abide/abide\\_II.html](http://fcon_1000.projects.nitrc.org/indi/abide/abide_II.html)

Table I

THE TABLE ILLUSTRATES THE PERFORMANCE OF OUR PROPOSED METHOD HYPERGALE AS COMPARED TO THE EXISTING STATE-OF-THE-ART APPROACHES. THE TRAIN AND TEST PROPORTIONS CONSIDERED FOR THE STUDY ARE 90% AND 10%, RESPECTIVELY. THE EXPERIMENTS ARE CONDUCTED FOR 5 DIFFERENT NON-OVERLAPPING PROPORTIONS OF DATA AND THE MEAN AND STANDARD DEVIATIONS ARE REPORTED.

Modality	Methods	Performance Metrics			
		Accuracy	AUC	Sensitivity	Specificity
<b>Traditional Methods</b>	SVM [31]	68.83± 2.44	68.07± 2.49	78.82± 2.65	57.31± 3.01
	Random Forest [32]	60.00± 5.55	58.80±6.11	70.81± 4.11	48.90±7.24
	Gradient Boosting	62.01± 2.99	61.45± 2.92	68.86± 4.54	54.05± 5.23
<b>Non-graph Methods</b>	ASD-Diagnet [8]	70.8 ±1.49	71.12 ±2.06	68.36 ±8.13	72.2 ±10.56
	BrainNetCNN [9]	67.32± 4.24	69.07± 3.05	68.89± 8.62	65.40± 11.56
<b>Graph based Methods</b>	GCN [13]	72.68±3.49	75.65± 3.57	<b>79.56± 8.42</b>	64.33± 9.65
	GAT [14]	68.53± 3.40	71.70± 4.11	65.78± 9.76	71.89± 9.75
	GraphSAGE [15]	71.22±2.55	74.64±4.60	75.43±17.88	66.61±2.56
<b>Transformer Based Methods</b>	Transformer [10]	67.80± 0.98	69.14± 1.87	62.99± 6.55	72.50± 4.07
	BrainNetTransformer [11]	71.22± 0.97	73.60± 2.38	67.70± 8.27	<b>74.29± 5.54</b>
<b>HyperGraphs (Ours)</b>	HyperGraphGCN	73.41±1.18	76.66±1.02	74.67±5.76	71.89±5.91
	HyperGALE (Ours)	<b>75.34± 0.47</b>	<b>77.03± 1.85</b>	76.39± 4.84	73.91± 5.58

structure and the associated weights, we define the hypergraph convolution operation as,

$$x_t^{(d+1)} = \sigma \left( \sum_{i=1}^N \sum_{j=1}^K \mathcal{H}_{tj} \mathcal{H}_{ij} W_{jj} x_i^{(d)} \Theta \right) \quad (1)$$

Here  $x_t^{(d)}$  is the embedding of the  $t^{\text{th}}$  vertex in the  $d^{\text{th}}$  layer. The  $\Theta$  is the weight matrix between two successive layers. Now we can eventually formulate the equation (1) into a matrix form as

$$X^{(d+1)} = \sigma \left( \mathcal{H} W \mathcal{H}^T X^{(d)} \Theta \right) \quad (2)$$

From the above equation the  $X^{(d)} \in \mathbb{R}^{N \times F^{(d)}}$  is the input of the  $d^{\text{th}}$  layer and the  $\Theta \in \mathbb{R}^{F^{(d)} \times F^{(d+1)}}$ . The equation (2) refers to a basic formulation that might lead to numerical instabilities with deepening layers causing gradients to vanish. Thus, to tackle this, one can adopt normalization approaches, such as symmetric normalization or row-normalization. In our line of research, we adopt the row-normalization approach as it provides directional propagation as in the below equation

$$X^{(d+1)} = \sigma \left( D^{-1} \mathcal{H} W B^{-1} \mathcal{H}^T X^{(d)} \Theta \right) \quad (3)$$

**Learnable Hyperedges and Gated Attention** In the equation (3) the weight matrix is not learnable. In such cases, the hypergraph will not be updated with respect to the samples. So our method even tries to learn the hyperedge weights matrix  $W$  and we represent it as  $\tilde{W}$  (refer to fig. 2). Successively, this information is passed through a gated attention network as formulated below,

$$\begin{aligned} A &= \sigma(\text{MLP}(X^{(d+1)})); \\ B &= \text{Tanh}(\text{MLP}(X^{(d+1)})); \\ \alpha &= \text{MLP}(A \odot B); \\ Z &= \alpha \odot X^{(d+1)} \end{aligned} \quad (4)$$

Where,  $\odot$  determines the element-wise product and  $\text{Tanh}(\cdot)$ ,  $\sigma(\cdot)$  are the nonlinear activation's respectively. In the equation (4),  $Z$  obliges our model to allocate necessary attention that are

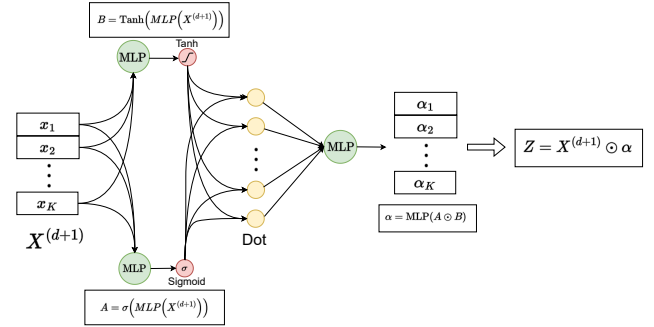


Figure 3. **Illustration of the Gated Attention Module.** GA module which learns  $\alpha$  iteratively (or numerically) from eq. (4), this  $\alpha$  vector is multiplied to get the final node features which is fed to the readout layer. [33].

crucial to interpreting the exact incidence of ASD [33]. This guides the hyperedge weight matrix to direct the importance to the essential nodes. Thus, it eventually tracks essential regions of the brain that are actually connected and injects the importance accordingly (refer to Fig. 3).

**Readout Mechanisms** The Readout methods produce an aggregation of node-level features to form graph-level representations. The standard readouts such as,  $\text{MAX}(\cdot)$  and  $\text{MEAN}(\cdot)$  underfit while learning on brain hypergraphs. So we experimented with adaptive readouts like SETTRANSFORMER and JANOSSY (permutation invariant) and MLP (permutation non-invariant). Thus, we deploy *Neural Readouts* where the hypothesis space of the aggregated representations is not permutation invariant. Also similar to Buterez *et al.* [34] we applied three variants of adaptive neural readouts, SETTRANSFORMER, JANOSSY and MLP readouts. We experimented with both permutation variant and invariant that are adaptive and embedded with permutation invariant learning with and without attention mechanisms [34]. After a detailed experiments we have seen MLP readouts outperform many adaptive and non-adaptive readouts. The ablations are detailed briefly in the results section. Our chosen readout is,

$$X^{(\text{Readout})} = \text{RELU}(\text{MLP}(Z)) \quad (5)$$

Finally, the total pipeline of our HyperGALE is described in the below Algorithm.1

---

**Algorithm 1: HYPERGALE**

---

**Input:** DATA

**Output:**  $\hat{y}$

$FC \leftarrow \text{SCHAEFERPARCELLATION}(\text{DATA})$

**for**  $i \leftarrow 1$  **to**  $epochs$  **do**

Hypergraph Creation:  $\mathcal{G}_{hyper}(V, \mathcal{H})$   
 $X^{(d+1)} \leftarrow \sigma\left(\mathcal{D}^{-1}\mathcal{H}\tilde{W}\mathcal{B}^{-1}\mathcal{H}^T X^{(d)}\Theta\right)$   
 $Z \leftarrow \alpha \odot X^{(d+1)}$   
 $X^{(\text{Readout})} \leftarrow \text{RELU}(\text{MLP}(Z))$   
 $\hat{y} \leftarrow \sigma(X^{(\text{Readout})})$

**return**  $\hat{y}$

---

IV. RESULTS AND DISCUSSION

In this section, we compare our proposed method with methods that are employed to provide significant performance for ASD classification. Later we determine the qualitative performance of HyperGALE in determining ASD.

A. Methods for Comparison

All the baseline experiments have been conducted on the dataset we have identified from ABIDE II and where necessary we have re-implemented the algorithms for reporting the comparative results in Table I. First, to observe the significance of statistical approaches the traditional machine learning methods such as Support Vector Machines, Random Forests, and Gradient Boosting Classifier (GBC) have been implemented. These models have been poorly performed due to the high variance nature of the data (refer Table I). Nevertheless, comparing among traditional methods, SVM gave better prediction performance.

Next, moving to the architectures using deep learning without transformer, the works [8], [9] have decent and better performance compared to traditional methods. Although, these methods have succeeded to provide jump in performance compared to that of traditional methods these models have high standard deviation and needs to be better in capturing the patterns that corresponds to ASD.

Next, we move to latest transformer architectures [10], [11] have achieved promising performance with less standard deviation in AUC and accuracy metrics. Although, having self-attention layers and OCREadout mechanisms, these methods do not provide significant performance.

Now, we benchmark the graph-based models [13]–[15]. As explained earlier, graph-based have actually performed well for ASD dataset [16] [17] [18]. Graph-based approaches on FC matrices are applied to understand interactions among regions of interest, but current methods struggle with higher-order proximity due to reliance on static dyadic edges.

Recent studies using Hypergraphs for ASD classification include Hypergraph U-Net [19] and multi-view HGNN [20] which use multiple modalities and thus we can't employ these

Table II

THE TABLE ILLUSTRATES THE PERFORMANCE HYPERGRAPH MODELS IN THE COMBINATIONS OF WITH AND WITHOUT GA AND LEARNED HE.

Methods		Performance Metrics			
Learned HEs	GA	Accuracy	AUC	Sensitivity	Specificity
W/o	W/o	73.41±1.18	76.66±1.02	74.67±5.76	71.89±5.91
W/o	With	74.39±1.21	<b>77.90±0.90</b>	67.78±1.11	<b>82.43±1.35</b>
With	W/o	73.74±1.39	77.15±3.80	68.10±7.20	81.15±6.56
With	With	<b>75.34±0.47</b>	77.03±1.85	<b>76.56±5.41</b>	73.86±5.41

methods for our study. Finally, we employed the hypergraph convolution methods named HyperGraphGCN [30] to compare with the hypergraph baseline. Although these methods have the added advantage of acquiring higher-order proximity, HyperGALE performs extensively on top of every model. In the next subsection, we explain all the experiments in detail and justify HyperGALE with extensive ablation studies.

B. Performance Discussion

Table I showcases that HyperGALE achieves notable performance, effectively justifying its design principles. The robustness of HyperGALE is confirmed in both accuracy and AUC metrics. A two-sample t-test comparing HyperGALE with HyperGraphGCN (a hypergraph-based baseline) reveals a significant difference in accuracy (t-Statistic: 3.40, p-Value: 0.0094), highlighting HyperGALE's superior performance in this regard. When compared with BrainNetTransformer, HyperGALE exhibits a highly significant improvement in accuracy (t-Statistic: 8.55, p-Value: 0.000027). Additionally, a significant enhancement is also observed in AUC (t-Statistic: 2.54, p-Value: 0.0345). These results highlight the efficacy of HyperGALE in handling functional connectivity (FC) patterns, particularly in Autism Spectrum Disorder (ASD) pattern identification.

While GCN demonstrates promising sensitivity, it suffers from fluctuating performance characterized by a high standard deviation. In terms of specificity, BrainNetTransformer excels, yet HyperGALE achieves comparable results. The superior performance of HyperGALE, especially in processing FC patterns, emphasizes its capability in delineating nuanced ASD patterns. Unlike transformer-based models that struggle with the utilization of FC as tokens and the physical understanding of attention mechanisms, HyperGALE adeptly processes these FC patterns, thereby capturing functional associations crucial in ASD diagnostics. This approach not only bolsters the model's accuracy and AUC but also enriches the understanding of ASD through cutting-edge machine learning techniques.

C. Generalizability

Our study employed a leave-one-site-out analysis across 16 different sites (refer Fig. 4) in the ABIDE-II dataset to evaluate the HyperGALE model's generalizability. This approach rigorously tested the model's performance in diverse settings, revealing insights into its applicability across various clinical environments. The analysis in Fig. 4 demonstrates varied performance metrics - across sites.

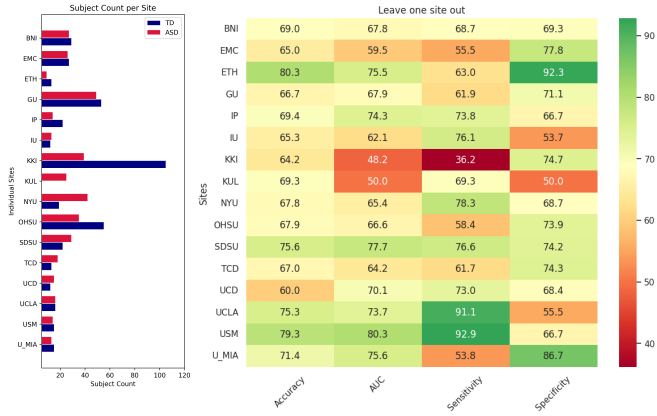


Figure 4. **Prediction performance across sites using a leave-one-site-out strategy.** The count of ASD and TD subjects from various sites are shown on (left) and various performance metrics are shown for each site on (right). Chance level performance is at 50%. Despite the challenges with site-specific variations in the number of samples, our model is still able to demonstrate credible between-site generalization performance, comparable to the results in Table I.

The results underscore the challenge of generalizing models in multi-site studies, highlighting the influence of site-specific factors such as data acquisition protocols and demographic variations. Performance discrepancies across sites suggest the need for further model enhancements, potentially through site-adaptive methodologies.

#### D. Gated Attention and Hyperedge Discussion

Table II demonstrates the impact of incorporating Learned Hyperedges (HE) and the Gated Attention (GA) module in hypergraph models, assessed under various configurations with and without these modules. One can observe that, with GA, the model is performing well in AUC and specificity metrics even in the absence of learnable HE. But, learnable HE and GA together actually obliges the model to have higher accuracy score and sensitivity. The sensitivity is helpful to predict the presence the ASD. Hence, both of these act as tandem and pivotal in identifying key ROI embeddings, thereby focusing on the most significant regions for predicting ASD. Furthermore, as GA highlights significant ROIs, and learned HE assign varying weights to different networks in brain parcellation, learning in this way helps the model to focus on distinct ROIs to provide significant performance.

The significance of learned HE and the GA module extends beyond performance; they are also crucial for enhancing the model’s interpretability in identifying biomarkers, a topic we will explore in detail in Section V.

#### E. Ablation Study

a) *Number of ROIs in each Hyperedge:* In our hypergraph convolution approach, hyperedges are formed by grouping ROIs based on connectivity, with the  $k$ -NN algorithm determining the number of ROIs in each hyperedge. The choice of the hyperparameter  $k$ , which dictates the ROI count per hyperedge, is crucial as it influences the overlap of

Table III  
THE TABLE ILLUSTRATES THE PERFORMANCE OF VARIOUS READOUT MECHANISMS ON OUR PROPOSED HYPERGALE MODEL.

Methods	Performance Metrics			
	Accuracy	AUC	Sensitivity	Specificity
MLP	<b>75.34</b>	<b>77.03</b>	<b>68.10</b>	81.15
Set Transformer	67.36	65.95	41.03	77.14
Janossy	62.96	58.08	63.16	62.79
Max	51.12	54.14	23.00	<b>97.30</b>
Mean	48.17	50.36	10.00	94.59

hyperedges, impacting the identification of active brain regions in ASD and TD subjects [35]. A lower  $k$  value might exclude vital information by limiting the ROIs per hyperedge, whereas a higher  $k$  risks adding non-significant connections and noise. Our empirical analysis as seen in Fig. 5, determined 40 to be the optimal ROI count in a hyperedge, balancing comprehensive coverage and minimal noise, crucial for accurate brain region representation in ASD and TD subjects.

b) *Number of Layers:* Our analysis shows that a single-layer hypergraph convolution is optimal for brain connectome analysis, as evidenced in Fig. 6. An increase in the number of layers led to a decline in performance, a phenomenon consistent with over-smoothing issues in graph convolutional networks (GCNs). This issue, as discussed in [36], [37], involves feature homogenization across layers, reducing the model’s ability to distinguish unique patterns.

The brain connectome’s structure, mainly consisting of ROIs one hop away from each other, supports our use of a single-layer approach. This structure allows for effective aggregation of essential information in the initial layer, making additional layers redundant. While various strategies have been proposed to address over-smoothing in deeper GNNs [38], [39], the architectural specifics of our dataset make these approaches less relevant, as our single-layer model adequately captures the necessary connectivity information.

c) *Readout Mechanisms:* Table III demonstrates that standard readouts like  $\text{MAX}(\cdot)$  and  $\text{MEAN}(\cdot)$  are less effective for brain hypergraphs. Supporting this, Buterez *et al.* [34] note that not all readouts suit every graph structure, especially in fully connected graphs like brain hypergraphs where permutation non-invariant readouts can be more effective.

The SETTRANSFORMER readout, used without positional encoding to preserve permutation invariance, contrasts with the permutation-invariant JANOSSY readout suggested by Murphy *et al.* [40]. However, in our study, MLP readouts provided superior embeddings for brain hypergraphs, aligning with findings by Alon *et al.* [41] that demonstrate their effectiveness in similar contexts. Hence, our framework utilized MLP readouts for optimal representation.

## V. INTERPRETABILITY DISCUSSION

Our analysis of brain connectome interactions unveils distinct neural patterns between ASD and TD subjects. Utilizing the Gated Attention module and learned hyperedge weights,

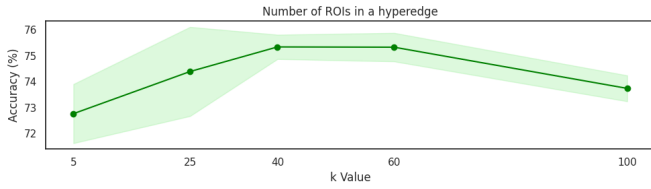


Figure 5. Changes in prediction accuracy with respect to change in number of ROIs in a hyperedge denoted by  $k$ . The optimal number of ROIs was found at  $k = 40$ .

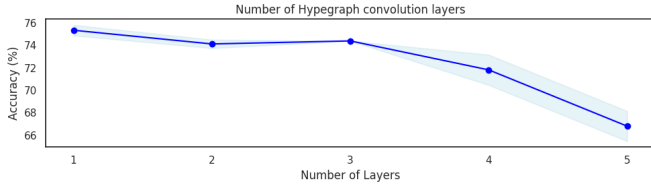


Figure 6. Changes in prediction accuracy with respect to change in the number of hypergraph convolution layers. A single-layer hypergraph convolution is found to be optimal.

we identified pivotal ROIs and observed how their interactions differ between ASD and TD individuals.

While Figs 7 (A) and (B) reveal a significant overlap in the top ROIs across both ASD and TD groups, it is the distinct connections among regions of these two groups that provide deeper insights and distinguish the two groups. In other words, despite sharing common ROIs, the way these regions interact within the neural network varies considerably between ASD and TD, reflecting the unique neural connectivity characteristics of ASD.

We identified the top 50 ROIs and categorized them into broader functional networks, each reflecting distinct aspects of the ASD classification. In the following we highlight the differences observed in the functional networks between ASD and TD. These include, Visual Processing Networks, which highlight atypical visual processing patterns in ASD [42]. The Limbic System indicates altered emotional and social processing through higher connectivity with the Default Mode Network (DMN) [43]. Executive Function and Attention Networks reveal disparities related to executive functioning and attention regulation challenges in ASD; and the Default Mode Network, where atypical connectivity patterns impact areas like theory of mind and self-awareness [43].

While Figs. 7 (A) and (B) indicate a substantial overlap in the top ROIs across both ASD and TD groups, it is their distinctive connectivity patterns that yield profound insights. This is particularly evident in the Limbic System, comprising of regions like Limbic TempPole and Limbic OFC. In ASD, we observe higher connectivity of these limbic regions with the DMN, as opposed to the balanced connections seen in TD. This higher linkage in ASD, as highlighted in Fig 7 (C) versus (D), is indicative of altered connectivity patterns in areas crucial for emotional processing and social interaction [43]. Similarly, in visual regions (RH Vis, LH Vis), we observe

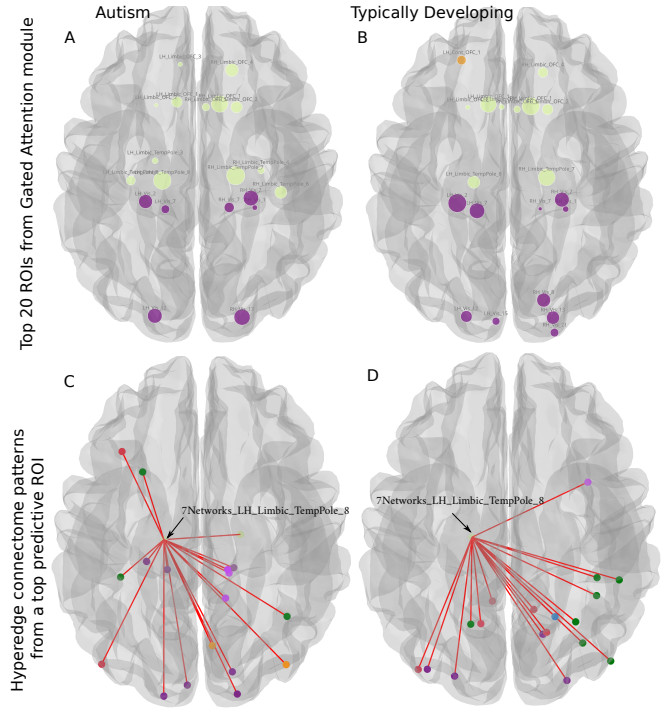


Figure 7. The interpretation of important ROIs and their connectivity obtained from GA module and learned hyperedge weights, respectively. (A) and (B) highlight the top 20 most important ROIs that emerged in ASD and TD subjects. (C) and (D) depict the discriminative hyperedge connectivity pattern of a common ROI in ASD and TD using dominant hyperedge based on  $\tilde{W}$ .

increased connectivity to DMN regions in ASD subjects [42], while TD had connections primarily within visual and attention networks.

These observations improve our understanding of ASD’s neural dynamics. The Limbic System’s enhanced DMN connectivity in ASD might underlie social and emotional processing challenges, while the varied connectivity in visual networks points to broader sensory and cognitive implications. Overall, our study extends beyond identifying shared ROIs, and discovering complex variations in neural interactions.

## VI. CONCLUSION

In this paper, we introduced HyperGALE, a novel hypergraph convolutional network enhanced with gated attention, specifically designed for ASD classification. Our comprehensive evaluation on the ABIDE-II dataset highlights HyperGALE’s outstanding performance, surpassing ML and graph-based approaches. HyperGALE’s capability to effectively capture complex higher-order graph intricacies and utilize learnable hyperedge weights has led to a better understanding of brain network dynamics. HyperGALE identifies critical ROIs for ASD and delineates how their connectivity patterns differ from those in TD subjects. This, not only promises improvements in clinical detection but also opens new avenues for research in neuroimaging and the development of targeted intervention strategies.

## REFERENCES

- [1] M. J. Maenner *et al.*, “Prevalence and characteristics of autism spectrum disorder among children aged 8 years—autism and developmental disabilities monitoring network, 11 sites, united states, 2020,” *MMWR Surveillance Summaries*, vol. 72, no. 2, p. 1, 2023.
- [2] L. Q. Uddin, K. Supekar, and V. Menon, “Reconceptualizing functional brain connectivity in autism from a developmental perspective,” *Frontiers in human neuroscience*, vol. 7, p. 458, 2013.
- [3] J. S. Nomi and L. Q. Uddin, “Developmental changes in large-scale network connectivity in autism,” *NeuroImage: Clinical*, vol. 7, pp. 732–741, 2015.
- [4] S. M. Smith *et al.*, “Correspondence of the brain’s functional architecture during activation and rest,” *Proceedings of the national academy of sciences*, vol. 106, no. 31, pp. 13040–13045, 2009.
- [5] J. Bathelt, H. M. Geurts, and D. Borsboom, “More than the sum of its parts: Merging network psychometrics and network neuroscience with application in autism,” *Network Neuroscience*, vol. 6, no. 2, pp. 445–466, 2022.
- [6] M. R. Arbabshirani, S. Plis, J. Sui, and V. D. Calhoun, “Single subject prediction of brain disorders in neuroimaging: Promises and pitfalls,” *NeuroImage*, vol. 145, pp. 137–165, 2017.
- [7] Y. Chen, J. Yan, *et al.*, “Adversarial learning based node-edge graph attention networks for autism spectrum disorder identification,” *IEEE Transactions on Neural Networks and Learning Systems*, p. 1–12, 2024.
- [8] T. Eslami, V. Mirjalili, A. Fong, A. R. Laird, and F. Saeed, “Asd-diagnet: a hybrid learning approach for detection of autism spectrum disorder using fmri data,” *Frontiers in neuroinformatics*, vol. 13, p. 70, 2019.
- [9] J. Kawahara *et al.*, “Brainnetcn: Convolutional neural networks for brain networks; towards predicting neurodevelopment,” *NeuroImage*, vol. 146, pp. 1038–1049, 2017.
- [10] A. Vaswani *et al.*, “Attention is all you need,” *Advances in neural information processing systems*, vol. 30, 2017.
- [11] X. Kan, W. Dai, H. Cui, Z. Zhang, Y. Guo, and C. Yang, “Brain network transformer,” *Advances in Neural Information Processing Systems*, vol. 35, pp. 25586–25599, 2022.
- [12] R.-A. Müller, N. Kleinhans, N. Kemmotsu, K. Pierce, and E. Courchesne, “Abnormal variability and distribution of functional maps in autism: an fmri study of visumotor learning,” *American Journal of Psychiatry*, vol. 160, no. 10, pp. 1847–1862, 2003.
- [13] T. N. Kipf and M. Welling, “Semi-supervised classification with graph convolutional networks,” *arXiv preprint arXiv:1609.02907*, 2016.
- [14] P. Veličković *et al.*, “Graph attention networks,” *arXiv preprint arXiv:1710.10903*, 2017.
- [15] W. Hamilton, Z. Ying, and J. Leskovec, “Inductive representation learning on large graphs,” *Advances in neural information processing systems*, vol. 30, 2017.
- [16] M. Cao, M. Yang, C. Qin, X. Zhu, Y. Chen, J. Wang, and T. Liu, “Using deepcn to identify the autism spectrum disorder from multi-site resting-state data,” *Biomedical Signal Processing and Control*, vol. 70, p. 103015, 2021.
- [17] A. Kazi, S. Shekarforoush, S. Arvind Krishna, H. Burwinkel, G. Vivar, K. Kortüm, S.-A. Ahmadi, S. Albarqouni, and N. Navab, “Inceptiongcn: receptive field aware graph convolutional network for disease prediction,” in *Information Processing in Medical Imaging: 26th International Conference, IPMI 2019, Hong Kong, China, June 2–7, 2019, Proceedings 26*, pp. 73–85, Springer, 2019.
- [18] D. Yao, M. Liu, M. Wang, C. Lian, J. Wei, L. Sun, J. Sui, and D. Shen, “Triplet graph convolutional network for multi-scale analysis of functional connectivity using functional mri,” in *Graph Learning in Medical Imaging: First International Workshop, GLMI 2019, Held in Conjunction with MICCAI 2019, Shenzhen, China, October 17, 2019, Proceedings 1*, pp. 70–78, Springer, 2019.
- [19] M. Lostar and I. Rekić, “Deep hypergraph u-net for brain graph embedding and classification,” *arXiv preprint arXiv:2008.13118*, 2020.
- [20] M. Madine, I. Rekić, and N. Werghe, “Diagnosing autism using t1-w mri with multi-kernel learning and hypergraph neural network,” in *2020 IEEE International Conference on Image Processing (ICIP)*, pp. 438–442, IEEE, 2020.
- [21] W. Shao, Y. Peng, C. Zu, M. Wang, D. Zhang, A. D. N. Initiative, *et al.*, “Hypergraph based multi-task feature selection for multimodal classification of alzheimer’s disease,” *Computerized Medical Imaging and Graphics*, vol. 80, p. 101663, 2020.
- [22] M. Liu, J. Zhang, P.-T. Yap, and D. Shen, “View-aligned hypergraph learning for alzheimer’s disease diagnosis with incomplete multi-modality data,” *Medical image analysis*, vol. 36, pp. 123–134, 2017.
- [23] J. Ji, Y. Ren, and M. Lei, “Fc-hat: Hypergraph attention network for functional brain network classification,” *Information Sciences*, vol. 608, pp. 1301–1316, 2022.
- [24] C. Craddock, S. Sikka, B. Cheung, R. Khanuja, S. S. Ghosh, C. Yan, Q. Li, D. Lurie, J. Vogelstein, R. Burns, S. Colcombe, M. Mennes, C. Kelly, A. Di Martino, F. X. Castellanos, and M. Milham, “Towards automated analysis of connectomes: The Configurable Pipeline for the Analysis of Connectomes (C-PAC),” *Frontiers in Neuroinformatics*, no. 42, 2013.
- [25] B. B. Avants, N. J. Tustison, G. Song, P. A. Cook, A. Klein, and J. C. Gee, “A reproducible evaluation of ants similarity metric performance in brain image registration,” *NeuroImage*, vol. 54, no. 3, pp. 2033–2044, 2011.
- [26] Y. Behzadi, K. Restom, J. Liau, and T. T. Liu, “A component based noise correction method (compcor) for bold and perfusion based fmri,” *NeuroImage*, vol. 37, no. 1, pp. 90–101, 2007.
- [27] A. Schaefer, R. Kong, E. M. Gordon, T. O. Laumann, X.-N. Zuo, A. J. Holmes, S. B. Eickhoff, and B. T. T. Yeo, “Local-Global Parcellation of the Human Cerebral Cortex from Intrinsic Functional Connectivity MRI,” *Cerebral Cortex*, vol. 28, no. 9, pp. 3095–3114, 2017.
- [28] O. Ledoit and M. Wolf, “A well-conditioned estimator for large-dimensional covariance matrices,” *J. Multivar. Anal.*, vol. 88, p. 365, 2004.
- [29] A. Abraham, F. Pedregosa, M. Eickenberg, P. Gervais, A. Mueller, J. Kossaifi, A. Gramfort, B. Thirion, and G. Varoquaux, “Machine learning for neuroimaging with scikit-learn,” *Frontiers in neuroinformatics*, vol. 8, 2014.
- [30] Y. Feng, H. You, Z. Zhang, R. Ji, and Y. Gao, “Hypergraph neural networks,” in *Proceedings of the AAAI conference on artificial intelligence*, vol. 33, pp. 3558–3565, 2019.
- [31] C. Cortes and V. Vapnik, “Support-vector networks,” *Machine learning*, vol. 20, pp. 273–297, 1995.
- [32] L. Breiman, “Random forests,” *Machine learning*, vol. 45, pp. 5–32, 2001.
- [33] M. Ilse, J. Tomczak, and M. Welling, “Attention-based deep multiple instance learning,” in *International conference on machine learning*, pp. 2127–2136, PMLR, 2018.
- [34] D. Buterez, J. P. Janet, S. J. Kiddle, D. Oglic, and P. Liò, “Graph neural networks with adaptive readouts,” *Advances in Neural Information Processing Systems*, vol. 35, pp. 19746–19758, 2022.
- [35] G. Lee, M. Choe, and K. Shin, “How do hyperedges overlap in real-world hypergraphs?—patterns, measures, and generators,” in *Proceedings of the web conference 2021*, pp. 3396–3407, 2021.
- [36] Q. Li, Z. Han, and X.-M. Wu, “Deeper insights into graph convolutional networks for semi-supervised learning,” in *Proceedings of the AAAI conference on artificial intelligence*, vol. 32, 2018.
- [37] D. Chen, Y. Lin, W. Li, P. Li, J. Zhou, and X. Sun, “Measuring and relieving the over-smoothing problem for graph neural networks from the topological view,” in *Proceedings of the AAAI conference on artificial intelligence*, vol. 34, pp. 3438–3445, 2020.
- [38] M. Liu, H. Gao, and S. Ji, “Towards deeper graph neural networks,” in *Proceedings of the 26th ACM SIGKDD international conference on knowledge discovery & data mining*, pp. 338–348, 2020.
- [39] G. Li, M. Müller, G. Qian, I. C. D. Perez, A. Abualshour, A. K. Thabet, and B. Ghanem, “Deepgcn: Making gcn go as deep as cnns,” *IEEE transactions on pattern analysis and machine intelligence*, 2021.
- [40] R. L. Murphy, B. Srinivasan, V. Rao, and B. Ribeiro, “Janosy pooling: Learning deep permutation-invariant functions for variable-size inputs,” *arXiv preprint arXiv:1811.01900*, 2018.
- [41] U. Alon and E. Yahav, “On the bottleneck of graph neural networks and its practical implications,” *International Conference on Learning Representations*, 2021.
- [42] M. V. Lombardo, L. Eyler, A. Moore, M. Datko, C. Carter Barnes, D. Cha, E. Courchesne, and K. Pierce, “Default mode-visual network hypoconnectivity in an autism subtype with pronounced social visual engagement difficulties,” *Elife*, vol. 8, p. e47427, 2019.
- [43] E. D. Bigler, D. F. Tate, E. S. Neeley, L. J. Wolfson, M. J. Miller, S. A. Rice, H. Cleavinger, C. Anderson, H. Coon, S. Ozonoff, *et al.*, “Temporal lobe, autism, and macrocephaly,” *American Journal of Neuroradiology*, vol. 24, no. 10, pp. 2066–2076, 2003.